Integrative Biology

Accepted Manuscript

This is an *Accepted Manuscript*, which has been through the Royal Society of Chemistry peer review process and has been accepted for publication.

Accepted Manuscripts are published online shortly after acceptance, before technical editing, formatting and proof reading. Using this free service, authors can make their results available to the community, in citable form, before we publish the edited article. We will replace this *Accepted Manuscript* with the edited and formatted *Advance Article* as soon as it is available.

You can find more information about *Accepted Manuscripts* in the Information for Authors.

Please note that technical editing may introduce minor changes to the text and/or graphics, which may alter content. The journal's standard Terms & Conditions and the Ethical guidelines still apply. In no event shall the Royal Society of Chemistry be held responsible for any errors or omissions in this *Accepted Manuscript* or any consequences arising from the use of any information it contains.

ROYAL SOCIETY OF CHEMISTRY

www.rsc.org/ibiology

Protein synthesis is a tightly regulated cellular process. Cancer cells, due to their metabolically unstable nature, usually have dysregulated protein synthesis pattern. Studying protein synthesis in cancer cells may shed light on basic cancer biology and facilitate the development of more effective therapy. Here we integrated microfluidic delivery of fluorescent tRNAs and Förster resonance energy transfer imaging to generate a unique method to visualize the production of proteins in single live cancer cells. Interesting and unique phenomena were observed such as the rapid disruption of protein synthesis pattern by puromycin and scattered distribution of tRNAs in mitotic cells. This method can be easily optimized for various cell lines and has the potential for broad applications in biomedical research.

Integrative Biology Accepted Manuscript

TITLE: Monitoring protein synthesis in single live cancer cells

Chengyi Tu[1], Loredana Santo[2,3], Yuko Mishima[2,3], Noopur Raje[2,3], Zeev Smilansky[4], Janet Zoldan[1*]

[1] *Department of Biomedical Engineering, University of Texas at Austin, Austin, TX*

[2] *Harvard Medical School, Boston, MA*

[3] *Center for Multiple Myeloma, Massachusetts General Hospital, Boston, MA*

[4] *Anima Cell Metrology, Bernardsville, NJ*

[*] **Corresponding Author**: Janet Zoldan, PhD; Phone: 512-471-4884; E-mail: zjanet@utexas.edu

Integrative Biology Accepted Manuscript

Abstract

Protein synthesis is generally under sophisticated and dynamic regulation to meet the ever-changing demands of a cell. Global up or down-regulation of protein synthesis, or the shift of protein synthesis location (as shown, for example, during cellular stress or viral infection) are recognized cellular responses to environmental changes such as nutrients/oxygen deprivation or to alterations such as pathological mutations in cancer cells. Monitoring protein synthesis in single live cells can be a powerful tool for cancer research. Here we employed a microfluidic platform to perform high throughput delivery of fluorescent labeled tRNAs into multiple myeloma cells with high transfection efficiency (~45%) and high viability (>80%). We show that the delivered tRNAs were actively recruited to the ER for protein synthesis, and that treatment by puromycin effectively disrupted this process. Interestingly, we observed scattered distribution of tRNAs in cells undergoing mitosis which has not been previously reported. Fluorescence lifetime analysis detected extensive FRET signals generated from tRNAs labeled as FRET pairs, further confirming that the delivered tRNAs were used by active ribosomes for protein translation. Our work demonstrates that microfluidic delivery of FRET labeled tRNA into living cancer cell can provide new insights into basic cancer metabolism and has the potential to serve as a platform for drug screening, diagnostics, or personalized medication.

Introduction

Protein synthesis, one of the most fundamental cellular processes, is usually under strict regulation. Cancer cells, due to their fast and uncontrolled growth, are generally more metabolically demanding than normal cells. The high metabolic demands of cancer cells are often coupled to their elevated protein synthesis rate.[1] In fact, changes in protein synthesis activity are always associated with the fate of cancer cells. Mutations in translation regulation (*e.g.* the hyperactivated mTOR pathway) in cancer cells can lead to elevated global protein production, promoting tumor progression and cell survival whereas attenuation of protein synthesis activity may indicate ongoing stress in cells or even apoptosis caused by adverse environment such as nutrient deprivation or hypoxia.[2-4] Numerous therapeutic strategies have been devised based on the high metabolic trait of cancer cells. Thus, monitoring protein synthesis activity in single live cancer cells can provide valuable insights into the basic biology of cancer cells, and in addition serve as a platform for diagnostics or for studying cellular responses (as manifested in aberrations to the process of protein synthesis) to various treatments.

Despite the clear need for single live-cell protein synthesis study, few commercially available assays allow such studies. In fact, most existing assays analyze fixed cells only. Förster resonance energy transfer (FRET) based protein synthesis monitoring (PSM) utilizes fluorescently labeled tRNAs (fl-tRNAs) as FRET pairs which generate FRET signals when they are immobilized in the A and P sites of active ribosomes and utilized during mRNA translation.[5-7] The PSM assay permits quantitative monitoring of protein synthesis in single live cells. Reported in 2011,[5] PSM has never been used with cells that are intrinsically hard to transfect such as primary cells and suspension cells, due to the difficulty of transfecting fl-tRNA and the long transfection times required by current protocols, compromising the value of the measured data. Here we demonstrate a novel, fast approach of delivering tRNA to live multiple myeloma (MM) cell**s** using a microfluidic

Integrative Biology Accepted Manuscript

based delivery device.[8] Instead of chemical vectors, this platform applies fast mechanical deformation to cells in a high throughput manner, generating transient pores in the cell membrane, allowing cargo (*e.g.,* proteins, microRNA and siRNAs) to flow in *via* passive diffusion.[8]

To demonstrate the advantage of combining microfluidic delivery with PSM, we chose MM cells as a model for hard-to transfect cells. MM cells are characterized by severely dysregulated protein synthesis, specifically, over-production of a single monoclonal paraprotein. The high rate of protein production leads to increased sensitivity of MM cells to proteasome inhibition, and drug sensitivity has been directly correlated with proteasome load.[9, 10] Thus, studying the protein synthesis activity in live MM cells is clinically relevant and may potentially shed lights on understanding drug response.

In this study, we integrated two state-of-art techniques, PSM and microfluidic delivery, to study protein synthesis activity in live U266 cells, an established MM cell line. We demonstrated efficient delivery of fl-tRNAs to U266 cells with high viability and showed localization of the fl-tRNAs to the endoplasmic reticulum (ER). Localization of fl-tRNAs was drastically disrupted by the treatment of puromycin, a protein synthesis inhibitor/ER stress inducer. Lastly, we successfully mapped out the protein synthesis activity in a single cancer cells using the fluorescence lifetime based FRET signal. This work shows that PSM can be applied to studying the protein synthesis activity in a hard-to-transfect cancer cell line at single-cell level. This technology may facilitate better understanding of cancer cell heterogeneity and may also serve as drug screening platform for identifying drugs targeting cancer metabolism, following cellular response to treatment, and novel diagnostics.

Materials and Methods

Cell culture

U266 cells (ATCC, USA) were cultured in RPMI-1640 media (ATCC, USA), supplemented with 10% fetal bovine serum (Gibco, USA), 2mM L-glutamine (Gibco, USA) and 1% penicillin/streptomycin (Corning, USA). Two days before transfection, cells were seeded at the density of $2.5x10^5$ cells/mL in 100 mm tissue culture plates. Before delivery, cells were spun down at 300g for 5 min and re-suspended in complete culture media (for FITC-Dextran delivery) or in RPMI-1640 basal media (for fl-tRNA delivery) to yield a final concentration of $2x10^6$ cells/mL.

Microfluidic delivery

Microfluidic chips (SQZ Biotech, USA) of various designs (10-7x1, 30-6x1, 10-7x5 and 10-9x1) were used to deliver 40 kDa FITC-Dextran (FITC-Dex) (Life Technologies, USA) or fluorescently labeled tRNAs (fl-tRNAs) (Anima Cell Metrology, USA). Fluorescent labeling of tRNA was performed as previously described.[11, 12] Briefly, Dihydrouridines of total tRNA from baker's yeast (Roche Diagnostics, Laval, Canada) were reduced with NaBH4 and labeled with Alexa Fluor488 and Alexa Fluor 555 (ThermoFisher scientific, USA) or Cy3 and Rhodamine 110 (GE healthcare, USA). Yeast tRNAs have been shown to be able to participate in protein synthesis in mammalian cells.[5] Delivery of FITC-Dex or fl-tRNAs was followed as

Integrative Biology Accepted Manuscript

previously described.[13] Briefly, U266 cell suspension (2x10^6 cells/mL), pre-filtered with a 35-µm cell strainer (Corning, USA) to remove cell clumps that can clog microfluidic chips, was mixed with FITC-Dex (0.2 mg/mL, final concentration) or fl-tRNAs (50 µg/mL, final concentration). The mixture was then passed through the microfluidic chips under desirable gas pressure (10 psi, 30 psi or 50 psi) and then allowed to recover at 37°C for 5-10 min. Cells were then further cultured or FACS analyzed.

FACS analysis

Transfected cells were washed twice with warm culture media to remove free dextran or fl-tRNA and re-suspended in 100 µL Dulbecco's phosphate-buffered saline. For viability assay, 5 µL of 7-AAD (eBioscience, USA) was added to the cell suspension 5 min before FACS measurements. FACS analysis was performed using AccuriC6 cytometer (BD Biosciences, USA). Data was analyzed with flowPlus and FlowJo software (Treestar, USA).

Live-cell staining

ER staining: Live-cell ER staining was performed with ER-tracker Green (Gibco, USA) according to manufacturer's guidelines. Briefly, cells were washed and re-suspended in Hank's balanced salt solution (HBSS) (Gibco, USA) containing 1 µM ER tracker. Following 20 min incubation at 37°C, cells were washed with HBSS, re-suspended in pre-warmed culture media and imaged with confocal microscopy (Zeiss, Germany).

Nuclear staining: Hoechst 33342 (Life Technologies, USA) was used for nucleus staining. Hoechst 33342 was directly added to the cells to the final concentration of 6 µg/mL and incubated at 37°C for 30 min prior imaging.

Tagging and detection of nascent proteins

Labeling and detection of nascent proteins in U266 cells was performed with Click-iT AF488 protein synthesis kit (Life technologies, USA). The procedure was performed according to manufacturer's guidelines. Briefly, O-propargyl-puromycin (OPP), an amino acid analog, was added to the U266 cell culture for 30 min followed by two PBS washes. The cells were then fixed with 4% paraformaldehyde (PFA, Polysciences, USA) for 15 min at room temperature, permeabilized with 0.25-0.5% triton X-100 (Amresco, USA) for 15 min and washed with PBS. Detection of OPP labeled nascent proteins was performed using the reaction cocktail containing Alexa fluor picolyl azide, copper protectant and reaction additives prepared as instructed. Subsequently, cells were rinsed with quenching reagents to stop the reaction followed by rinsing twice with PBS before confocal imaging.

Drug treatment

Puromycin (Sigma-Aldrich, USA, final concentration of 2 mM) or cycloheximide (Sigma-Aldrich, final concentration of 0.1 mg/mL) was added to U266 cells transfected with Alexa Fluor 555 (AF555)-tRNA immediately after transfection. The cells were incubated for 4 hours at 37°C and imaged to analyze changes in fl-tRNA localization.

Confocal microscopy

All live-cell imaging was performed with Zeiss spinning disk confocal microscope with an apochromat 100 x, 1.4 numerical aperture oil immersion objective and EMCCD iXon3 897 camera (Andor Technology; Belfast, UK). Exposure

Integrative Biology Accepted Manuscript

time was 200 ms. Cells were seeded on poly-d-lysine-coated 35 mm glass-bottom petri-dishes (Mat Tek, USA) at least 15 min before imaging to allow for the cells to sink to the bottom surface. Co-localization of AF555-tRNA or Cy3 labeled control siRNA (Life Technologies, USA) with ER staining was analyzed with ZEN software and the Pearson's correlation coefficient was calculated by the software. For each group, 20 cells were used for the calculation.

Fluorescence lifetime measurements

U266 cells were transfected with both AF488-tRNAs (50 µg/mL) and AF555-tRNA (200 µg/mL) as a FRET pair using 30-6x1 chip under 30 psi pressure. Alternatively, U266 cells were transfected with only AF488-tRNAs under the same conditions. For internal control, we added free AF488 dyes into the AF488-tRNA sample (1:1, mole/mole). These free AF488 dyes would be delivered into the cytosol but can not be recruited into ER so they should not be quenched and thus serve as an internal control. Upon transfection, the cells were washed and seeded in a 96-well plate (corning, USA) and incubated for 3.5 hours. Cells were re-suspended in cold fresh media and mixed with matrigel (corning, USA) at a ratio of 1:1 (v/v). The solution was transferred to a glass-bottom petri-dish and allowed to gel at 37℃ for 10 min. The imaging procedure was as previously described with minor changes in instrumentation.[14] Briefly, the sample was illuminated with a 488 nm picosecond laser pulse operating at a repetition rate of 50 MHz. Images were obtained by scanning the sample with a step size of 200-500 nm using a piezoelectric-driven translation stage (Mad City Labs, USA). Fluorescence signal was focused onto GaAsP photomultiplier tubes (Hamamatsu, Japan). The output was amplified and analyzed for time-correlated single-photon counting (TCSPC). The fluorescence lifetime of the donor is directly inversely correlated with FRET efficiency. The quenching was computed as the difference between the fluorescence lifetime of the region of interest and the cytosol.

Results and Discussion

Optimization of microfluidic delivery

Multiple Myeloma cells, as suspension cells, are difficult to transfect using conventional techniques such as liposomal delivery or electroporation. Moreover, most commercially available transfection kits are designed for DNA or microRNA delivery but not specifically for tRNA. Microfluidic delivery as a novel high throughput delivery methodology provides a functional alternative to chemical transfection. In order to identify optimal conditions for delivering macromolecules into U266 cells, we started by optimizing transfection using 40 kDa FITC labeled dextran (FITC-Dex) as a model molecule, since it is of comparable size to fl-tRNAs (~ 25 kDa). Because microfluidic delivery is largely dependent on passive diffusion, the size of a cargo molecule plays a more important role than its biochemical properties. Thus, we reasoned that FITC-Dex would be an appropriate model molecule for fl-tRNA. We tested a range of chip designs with various gas pressure values. Specifically, for the microfluidic chips, we can vary the length and width of the constrictions, and the number of consecutive constrictions (Fig 1A). For example, a 10-7x1 chip has 1 constriction per channel and it is 10 µm in length and 7 µm in width. Specifically, we employed 4 different chip designs: 10-7x1, 30-6x1, 10-9x1 and 10-7x5 using 3 different pressure values: 10 psi, 30 psi and 50 psi. Using confocal microscopy imaging, we confirmed that FITC-Dex was delivered into live U266 cells efficiently. As FITC-Dex has no functionality it is dispersed uniformly inside the cells (Fig.1B).

Integrative Biology Accepted Manuscript

Overall, and in agreement with previous reports,[13] our FACS analysis shows that transfection efficiency increased with narrower constrictions, more consecutive constrictions and higher gas pressure (Fig.1C), presumably due to higher shear stress and normal stress applied to the cells. However, as expected, higher transfection efficiency was also accompanied by increased cell death (Fig.1D). Using the10-7x5 chip, for instance, resulted in increasing transfection efficiency, 17%, 59% and 67% under increasing pressure flow of 10 psi, 30 psi, and 50 psi respectively, but also caused significant cell death (*e.g.*, 45% cell death at 50 psi). Transfection using the 10-9x1 chip, in contrast, led to less than 2% cell loss even at 50 psi pressure, but also had very inefficient transfection (*e.g.*, <6%) (Fig.1C, blue square). We determined that 30-6x1chip design is most desirable for our experiment, generating high transfection efficiency (36%, 56% and 73% under 10 psi, 30 psi, and 50 psi respectively) (Fig.1C, orange cross) and minimally compromising cell viability (>80%).

fl-tRNA delivery and sub-cellular localization

We first set out to apply conventional transfection methods to deliver fl-tRNAs into U266 cells. We introduced fl-tRNA (rhodamine 110 or Cy3 labeled) into U266 cells employing a commonly used INTERFERin transfection protocol. After transfection, the cells were cytospun onto microscope slides, fixed and then imaged. The two fl-tRNAs were highly colocalized (Fig.S1A). Additionally, we observed a significant colocolization between Cy3-tRNA and calnexin, a marker of endoplasmic reticulum (ER), the main site of protein synthesis, indicating that the transfected fl-tRNA participates in translation (Fig.S1B). As our goal was to image live cells, we repeated INTERFERin transfection of U266 cells this time with Alexa labeled tRNAs (AF555-tRNAs) to increase fl-tRNA brightness and photo-stability and performed live-cell imaging. Notably, delivered AF555-tRNAs formed clustering pattern outside nucleus (Fig.S2A), a phenomena not observed when cells were imaged after cytospinning and fixation, suggesting that fixation or cytospinning could have altered the cell morphology along with fl-tRNA localization. Despite successful delivery of fl-tRNAs into U266 cells using INTERFERin transfection, the efficiency was relatively low (<10% cells transfected as measured by FACS) (Fig.S2B) and time consuming, requiring 6-7 hours of incubation time. In contrast, as we demonstrate in the following paragraphs, microfluidic delivery is faster and more effective. Additionally upon optimization, microfluidic delivery was shown to confer better control over the amount of molecules delivered into cells.[8, 13]

Towards overcoming the limitations of low transfection efficiency, we set out to use the condition identified in the optimization study (30-6x1, 30 psi), using the microfluidic device to deliver AF555-tRNAs into U266 cells. The microfluidic delivery significantly increased transfection efficiency to 45%, while maintaining high cell viability (> 80%). Although transfection efficiency with AF555-tRNA was slightly lower than the efficiency with FITC-Dex (56%). This decrease in efficiency can be explained, at least in part, by the higher labeling ratio of FITC-Dex (5:1, FITC: Dex) compared to AF555-tRNA (1:1, AF555: tRNA). Using fluorescence reading in combination with FACS, we roughly estimated that on average around 1.8×10^7 fl-tRNAs were delivered into each cell (Fig.S3). Previously, the total amount of endogenous tRNA molecules in a eukaryotic cell was estimated to be ~10^8.[15] Therefore, we reasoned that the quantity of fl-tRNAs we introduced *via* microfluidic delivery into U266 cells is sufficient to provide protein synthesis measurements while minimally altering cell behavior. Confocal imaging revealed successful delivery of fl-tRNAs to live U266 cells while significantly reducing the transfection duration. Delivered AF555-tRNAs formed clusters outside the nuclei (Fig.2) similar

Integrative Biology Accepted Manuscript

to the patterns observed when the fl-tRNAs were delivered *via* INTERFERin. (Fig.S2A) Using live-cell ER staining, we found that AF555-tRNAs were specifically localized to the ER (Fig.3A, upper panel). As a negative control, we delivered Cy3-siRNA with scrambled sequence to U266 cells using the same conditions. The Cy3-siRNA was randomly dispersed within the cytosol and did not form clusters (Fig.3A, lower panel). Specifically, Cy3-siRNA co-localization with ER staining was significantly lower (by nearly 50%) than AF555-tRNA as quantified by Pearson coefficient (Fig.3B), suggesting that the clustering of the fl-tRNAs was not a result of random aggregation and that delivered fl-tRNAs were recruited to the ER.

Furthermore, Hoechst staining easily identified mitotic cells by the absence of nuclear membrane and condensation of chromosomes (Fig.4A). Interestingly, the subcellular localization of AF555-tRNAs was drastically different in the mitotic cells than non-mitotic cells. Instead of forming clustering patterns, the fl-tRNAs were scattered over the entire cytosol (Fig.4A), implying reduced recruitment of fl-tRNAs into ER. This observation aligns with the well-known fact that rate of protein synthesis during mitosis in eukaryotic cells drops to only 20%-30% of their interphase level.[16] To validate that the change of fl-tRNA distribution in mitotic cells was due to decreased protein synthesis activity, we utilized a commercially available protein synthesis assay kit. The kit utilizes amino acid analog (O-propargyl-puromycin, OPP) to tag newly synthesized peptide chains and thus to quantify the proteins being made within the time of incubation. Although it requires cell fixation and permeabilization, applying this assay kit to U266 cells allowed visualization of newly synthesized proteins. In nearly all non-mitotic cells, most nascent proteins were found outside the nucleus forming clustering patterns (Fig.4B, upper panel), indicating that these cells exhibit highly localized protein synthesis activity, and thus aligning with our observation of fl-tRNA clustering. In contrast, very few nascent proteins or the clustering pattern were observed in mitotic cells (Fig.4B, lower panel). Collectively, these results demonstrated that the clustering pattern of delivered fl-tRNAs was due to active recruitment for protein synthesis and disruption of this pattern, as observed in mitotic cells, was in fact caused by the down-regulation of protein synthesis activity.

Effects of drug treatment on fl-tRNA sub-cellular localization

To demonstrate the importance of monitoring protein synthesis in MM cells, we perturbed our system using a panel of drugs targeting protein synthesis machinery. As MM cell are at high basal ER stress due to extensive immunoglobulin production and build-up of misfolded proteins, these cells have to maintain a delicate unfolded protein response (UPR) balance that favors survival. Puromycin is a translation inhibitor that competitively binds to the A site of ribosomes and causes the release of the nascent proteins. Puromycin has been used as an effective ER stress inducer,[17, 18] presumably due to the generation of immature nascent peptides. We first transfected U266 cells with AF555-tRNA, followed by treatment with 2 mM puromycin for 4 hours. The fl-tRNAs formed clusters outside nucleus prior to treatment (Fig.5, upper panel). Yet, upon short puromycin treatment, these fl-tRNA clusters broke up and dispersed throughout the cytosol (Fig.5, middle panel). In fact, the co-localization between fl-tRNAs and ER was significantly reduced upon a short 30 min puromycin treatment (Fig.S4). We infer that puromycin prevents clustering of fl-tRNA in the ribosome as a rapid way to decrease protein synthesis, demonstrating the sensitivity of the PSM assay. This observation also demonstrates that the fl-tRNAs were functional and recruited to ribosomes for protein synthesis upon delivery. In contrast,

Integrative Biology Accepted Manuscript

cycloheximide, another protein synthesis inhibitor, which acts by blocking the elongation step of translation, had minimal effects on the subcellular localization of the fl-tRNAs in U266 cells (Fig.5, lower panel), in accordance with a previous report which indicated that cycloheximide trapped fl-tRNAs inside ribosomes.[5] Yet, as high immunoglobulin production levels sensitize U266 cells to ER stress and to proteasome inhibitors such as bortezomib, reducing production of these paraproteins should result in reduced sensitivity to bortezomib treatment. Indeed, the effectiveness of bortezomib treatment to U266 cells was reduced upon subjecting these cells to cycloheximide, an inhibitor of protein biosynthesis. Addition of 250 nM cycloheximide to U266 cells increased cell viability to 87% compared to 70% of cells treated with only bortezomib. Furthermore, this phenomenon exhibits a dose response (*i.e*. a higher dose of 500 nM cycloheximide further increased cell viability to 94%) (Fig.S5), in accordance with previous reports,[19] correlating ER sensitivity of MM cells with immunoglobulin production levels. These results demonstrate the significance of monitoring protein synthesis in MM cells to unravel drug sensitivity and resistance.

Mapping protein synthesis activity in single live cell by fluorescence lifetime FRET (FLIM-FRET)

To further verify that the fl-tRNA actively functions in protein synthesis, we set out to perform FLIM-FRET measurements of AF488 within live single U266 cells (Fig.6). FLIM-FRET measurement circumvents most pitfalls often encountered when using intensity based FRET such as bleed-through between channels and direct excitation of the acceptor, thus it is a reliable way to confirm the presence of FRET. Briefly, as a pair of AF488-tRNA and AF555-tRNA is immobilized on the active mRNA in the ribosome, the two fl-tRNAs would be in close proximity (~5 nm) causing AF488 to be partially quenched due to FRET. Therefore, we anticipate a decrease in the AF488 fluorescence lifetime (Fig.6A). To examine changes in AF488 fluorescence lifetime, we delivered AF488-and AF555-tRNAs simultaneously as a FRET pair or AF488-tRNAs alone to U266 cells using the same condition (30-6x1 chip, 30 psi) as previous experiments. AF488- and AF555-tRNAs were highly co-localized and both formed clustering pattern outside nucleus (Fig.6B). Since intracellular environment is complex and there are numerous factors such pH and other cellular proteins that may quench fluorophores, we then added free AF488 dyes into AF488-tRNA sample (1:1, mole/mole). These free dyes would be delivered into cytosol along with fl-tRNAs but can not be recruited into ER, so the lifetime of their fluorescence (from the cytosol) would serve as an appropriate internal control.

Using a custom-built time correlated single photon counting (TCSPC) microscope, we generated a fluorescence lifetime heatmap of single live U266 cells for green fluorescence (AF488) by step-wise scanning. The AF488-tRNAs in the cluster pattern (white square) exhibited significantly shorter fluorescence lifetime (~ 2.7 ns) than that of outside of the pattern (~3.3 ns), indicating the presence of FRET signal (Fig.6C). Notably, the fluorescece lifetime of free AF488-tRNAs in culture media was measured at around 4.1 ns, suggesting that the intracellular environement can non-specifically quench fluorescence and also highlighting the importance of internal control. To quantify the quenching of AF488 inside the cluster pattern, we computed the difference between the fluorescence lifetime from inside the cluster pattern (white square) and from the cytosol. When both donor (AF488-tRNAs) and acceptor (AF555-tRNAs) were delivered, the lifetime decrease was around 0.57 ns (Fig.6D). Interestingly, when only the donor was delivered, there was although smaller still a significant decrease of lifetime of around 0.36 ns (Fig.6d). A reasonable explaination for this quenching in absence of

Integrative Biology Accepted Manuscript

acceptor could be homo-FRET between two closely immobilized AF488-tRNAs inside a ribosome. In fact, the homo-FRET between AF488 molecules has been explored by researchers to quantify the oligomer stoichiometry of membrane proteins.[20]

Overall, these results further confirm that the delivered fl-tRNAs were recruited to ER-bound ribosomes for protein synthesis. Though it is theoretically possible that FRET can also be generated as a result of dye aggregation, we ruled out this possibility based on the fact that the fl-tRNA localization could be altered by specific drug treatment that targets protein synthesis (*e.g.*, puromycin, Fig.5).

Conclusions

Protein synthesis is a complex biological process fundamental to all living cells. Numerous technologies have been developed aiming to quantify or visualize this intricate process. Isotopic labeling of amino acids (*e.g.*, ^{3}H-phenyalanine or ^{35}S-methionine) is a classical technique that enables researchers to quantify newly synthesized protein and has been extensively used for *in vivo* measurement of muscle protein synthesis.[21, 22] Despite the success achieved by this technique, it is usually time consuming, expensive and does not allow for single-cell nor live-cell measurement.[23] Alternatively, a nonradioactive assay based on FACS, called surface sensing of translation (SUnSET), utilizes puromycin to label nascent proteins and allows both quantification of population activity and direct visualization of protein synthesis in individual cells.[24] However, this technique requires fixation of cells and therefore is not applicable to monitoring the dynamic change of protein synthesis activity in live cells. A more recent technique based on stimulated Raman scattering microscopy (SRS) employs deuterium-labeled amino acids to detect the nascent proteins, allowing for live single cell measurement with spatial information regarding where the nascent proteins are located.[25]

Though the above mentioned methods have been proven to be useful, most of them (pulse chase, amino acid labeling, ribosome profiling) cannot monitor protein synthesis in live cells nor provide patient specific information by addressing the clonal heterogeneity of patient derived cells. PSM offers several unique advantages. First, instead of detecting signals from nascent proteins, it tracks signals from fl-tRNAs in active ribosomes, keeping the protein synthesis activity and the synthesized proteins unchanged, and thus enables direct monitoring of mRNA translation activity in live cells. Second, PSM allows for a longer time window of study since it does not measure nascent proteins. Technically, the time window is only limited by the photostability of the fluorescent dyes or stability of the fl-tRNAs (about 72 hours). In addition, this assay is relatively easy and fast, essentially comprising of only two steps: fl-tRNA delivery and imaging. Lastly, this assay may help researchers to depict a spatial map of protein synthesis activity in single live cells. For instance, we may potentially be able to distinguish protein synthesis in ER versus in cytosol using this assay, which can facilitate better understanding of how cells regulate protein synthesis to better cope with various environmental changes.

As cancer metabolism gains scientific attention, and numerous new cancer drugs target the protein translation apparatus and impact protein synthesis rates, an assay that can measure these rates in high throughput manner provides a clear advantage. Such an assay could be used to screen for drugs that target the protein synthesis process

Integrative Biology Accepted Manuscript

and assist in personalization of medication and treatment. Here we provided a proof of concept that PSM has the potential to serve as such an assay and become a surrogate tool for drug sensitivity. Specifically, we demonstrate that co-delivery of fl-tRNA is achievable with high efficiency in U266 cells and protein synthesis activity of individual cells can be mapped out in real-time using FRET signal generated by fl-tRNAs. Delivery can be easily optimized to other hard-to transfect cells by changing the chip constriction parameters and flow parameters. Moreover, PSM is a highly specific assay; delivered fl-tRNAs localize to the ER, forming characteristic clustering patterns; and when switching from bulk labeled fl-tRNA to specifically selected isoacceptor pairs, could monitor the synthesis of specific proteins.[26] These clustering patterns are unique to fl-tRNAs, and not observed upon Cy3 labeled siRNA delivery or in mitotic cells. Furthermore, clustering patterns of delivered fl-tRNA are sensitive to changes in protein synthesis rates and drug treatment (4 hr treatment with puromycin was sufficient to disrupt these patterns). Therefore, we concluded the fl-tRNAs are indeed inside ribosomes for protein synthesis. Taken together, these results demonstrate the unique data that becomes available with PSM. Future studies will focus on PSMs critical role in underpinnings of tumor metabolism and its drug sensitivity.

Acknowledgement

We would like to thank Dr.Jeanne Stachowiak for kindly providing access to the confocal microscope and expertise on fluorescence imaging. We would also like to acknowledge Wilton Snead for his help with fluorescence lifetime FRET imaging.

Conflict of Interest

Z.S. has a financial interest in Anima Cell Metrology, Ltd.

References

1. S. C. Dolfi, L. L. Chan, J. Qiu, P. M. Tedeschi, J. R. Bertino, K. M. Hirshfield, Z. N. Oltvai and A. Vazquez, *Cancer & metabolism*, 2013, **1**, 20.
2. M. Holcik and N. Sonenberg, *Nat. Rev. Mol. Cell Biol.*, 2005, **6**, 318-327.
3. C. Koumenis, C. Naczki, M. Koritzinsky, S. Rastani, A. Diehl, N. Sonenberg, A. Koromilas and B. G. Wouters, *Mol. Cell. Biol.*, 2002, **22**, 7405-7416.
4. H. Y. Jiang and R. C. Wek, *J. Biol. Chem.*, 2005, **280**, 14189-14202.
5. S. Barhoom, J. Kaur, B. S. Cooperman, N. I. Smorodinsky, Z. Smilansky, M. Ehrlich and O. Elroy-Stein, *Nucleic Acids Res.*, 2011, **39**, e129.
6. C. Chen, B. Stevens, J. Kaur, D. Cabral, H. Liu, Y. Wang, H. Zhang, G. Rosenblum, Z. Smilansky, Y. E. Goldman and B. S. Cooperman, *Mol. Cell*, 2011, **42**, 367-377.
7. J. Q. Liu, M. Pampillo, F. Guo, S. X. Liu, B. S. Cooperman, I. Farrell, D. Dahary, B. S. Gan, D. B. O'Gorman, Z. Smilansky, A. V. Babwah and A. Leask, *J. Cell. Physiol.*, 2014, **229**, 1121-1129.
8. A. Sharei, J. Zoldan, A. Adamo, W. Y. Sim, N. Cho, E. Jackson, S. Mao, S. Schneider, M. J. Han, A. Lytton-Jean, P. A. Basto, S. Jhunjhunwala, J. Lee, D. A. Heller, J. W. Kang, G. C. Hartoularos, K. S. Kim, D. G. Anderson, R. Langer and K. F. Jensen, *Proc Natl Acad Sci U S A*, 2013, **110**, 2082-2087.
9. S. Meister, U. Schubert, K. Neubert, K. Herrmann, R. Burger, M. Gramatzki, S. Hahn, S. Schreiber, S. Wilhelm, M. Herrmann, H. M. Jack and R. E. Voll, *Cancer Res.*, 2007, **67**, 1783-1792.
10. G. Bianchi, L. Oliva, P. Cascio, N. Pengo, F. Fontana, F. Cerruti, A. Orsi, E. Pasqualetto, A. Mezghrani, V. Calbi, G. Palladini, N. Giuliani, K. C. Anderson, R. Sitia and S. Cenci, *Blood*, 2009, **113**, 3040-3049.
11. D. Pan, H. Qin and B. S. Cooperman, *RNA*, 2009, **15**, 346-354.
12. J. Kaur, M. Raj and B. S. Cooperman, *RNA*, 2011, **17**, 1393-1400.

Integrative Biology Accepted Manuscript

13. A. Sharei, R. Poceviciute, E. L. Jackson, N. Cho, S. Mao, G. C. Hartoularos, D. Y. Jang, S. Jhunjhunwala, A. Eyerman, T. Schoettle, R. Langer and K. F. Jensen, *Integr. Biol. (Camb.)*, 2014, **6**, 470-475.
14. J. C. Stachowiak, E. M. Schmid, C. J. Ryan, H. S. Ann, D. Y. Sasaki, M. B. Sherman, P. L. Geissler, D. A. Fletcher and C. C. Hayden, *Nat. Cell Biol.*, 2012, **14**, 944-949.
15. R. A. Weinberg and S. Penman, *J. Mol. Biol.*, 1968, **38**, 289-304.
16. J. E. Celis, P. Madsen and A. G. Ryazanov, *Proc Natl Acad Sci U S A*, 1990, **87**, 4231-4235.
17. M. Hammadi, A. Oulidi, F. Gackiere, M. Katsogiannou, C. Slomianny, M. Roudbaraki, E. Dewailly, P. Delcourt, G. Lepage, S. Lotteau, S. Ducreux, N. Prevarskaya and F. Van Coppenolle, *Faseb J*, 2013, **27**, 1600-1609.
18. V. Croons, W. Martinet, A. G. Herman and G. R. De Meyer, *J. Pharmacol. Exp. Ther.*, 2008, **325**, 824-832.
19. S. Meister, U. Schubert, K. Neubert, K. Herrmann, R. Burger, M. Gramatzki, S. Hahn, S. Schreiber, S. Wilhelm, M. Herrmann, H. M. Jack and R. E. Voll, *Cancer Res*, 2007, **67**, 1783-1792.
20. A. M. Melo, A. Fedorov, M. Prieto and A. Coutinho, *Phys. Chem. Chem. Phys.*, 2014, **16**, 18105-18117.
21. E. J. Barrett, J. H. Revkin, L. H. Young, B. L. Zaret, R. Jacob and R. A. Gelfand, *Biochem. J.*, 1987, **245**, 223-228.
22. P. J. Garlick, M. A. McNurlan and V. R. Preedy, *Biochem. J.*, 1980, **192**, 719-723.
23. C. A. Goodman and T. A. Hornberger, *Exerc. Sport Sci. Rev.*, 2013, **41**, 107-115.
24. E. K. Schmidt, G. Clavarino, M. Ceppi and P. Pierre, *Nature methods*, 2009, **6**, 275-277.
25. L. Wei, Y. Yu, Y. Shen, M. C. Wang and W. Min, *Proc Natl Acad Sci U S A*, 2013, **110**, 11226-11231.
26. S. Barhoom, I. Farrell, B. Shai, D. Dahary, B. S. Cooperman, Z. Smilansky, O. Elroy-Stein and M. Ehrlich, *Nucleic Acids Res.*, 2013, **41**, e177.

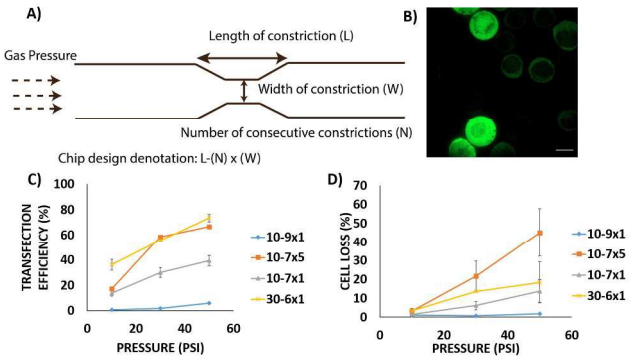

Figure 1. Optimization of delivery condition using 40 kDa FITC-Dex. (A) Microfluidic chips of various length, constriction width and number of constrictions and various gas pressure were used to deliver 40 kDa FITC-Dex into U266 cells; (B) a representative image of U266 cells successfully transfected with FITC-Dex; (C) transfection efficiency was quantified by FACS. Increased pressure, narrower constrictions and more consecutive constrictions lead to higher transfection efficiency; (D) cell viability was measured by 7-AAD and is generally inversely correlated with transfection efficiency. Scale

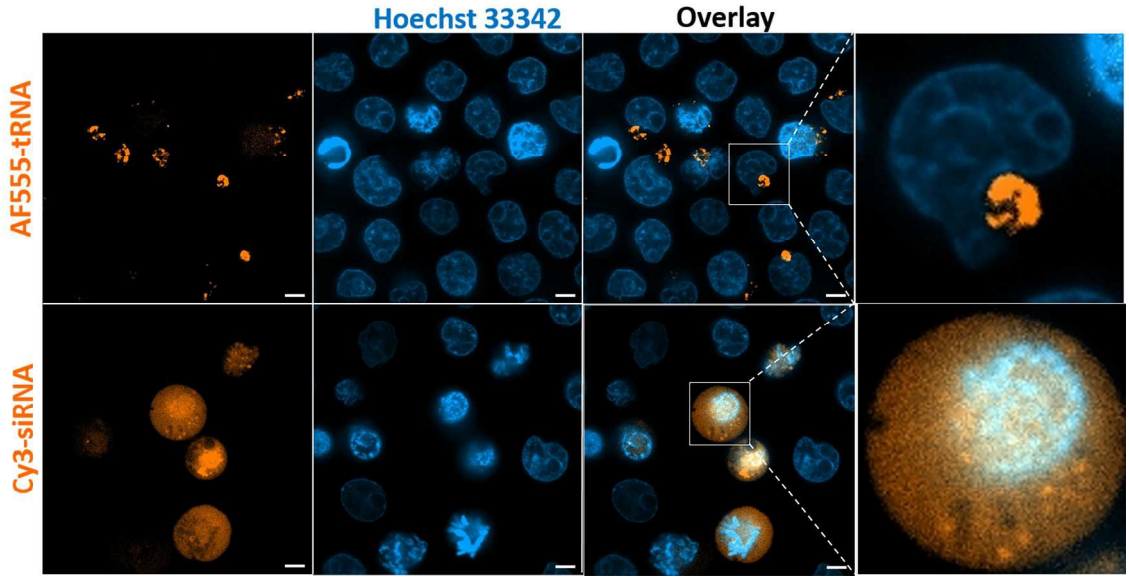

Integrative Biology Accepted Manuscript

Figure 2 Delivery of AF555-tRNA and negative control Cy3-siRNA into live U266 cells. AF555-tRNAs or Cy3-siRNAs (with scrambled sequence) were delivered into U266 cells with 30-6x1 chip at 30 psi. The transfected AF555-tRNAs were actively recruited to form clustering patterns outside nucleus whereas Cy3-siRNA was distributed inside the cells without any specific pattern, indicating the specificity of the pattern formation. Scale bar: 5 µm.

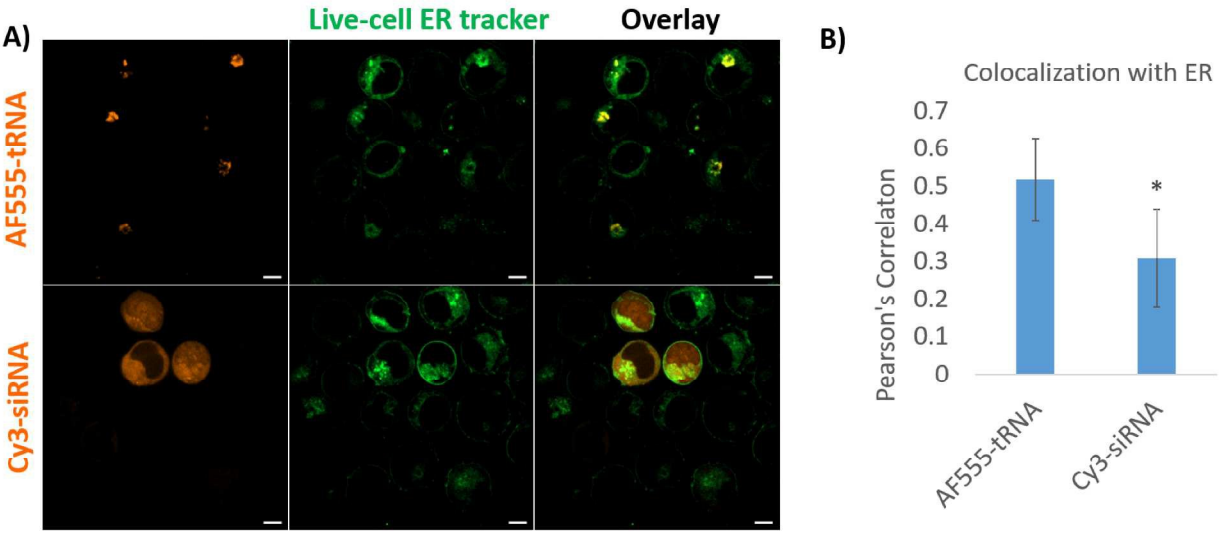

Figure 3 Co-localization of AF555-tRNA with live cell ER tracking. (A) U266 cells transfected with AF555-tRNA or Cy3-siRNA were stained with live cell ER tracker; (B) co-localization with ER was quantified using ZEN software. For each group, 20 cells were used to calculate Pearson's correlation. *p<0.01. Scale bar: 5 µm.

Integrative Biology Accepted Manuscript

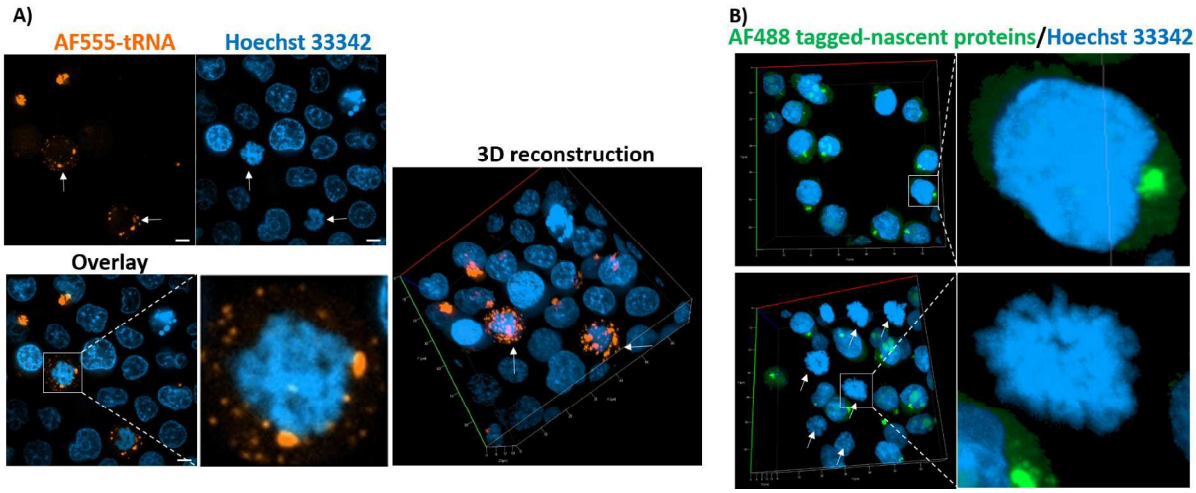

Figure 4 Protein synthesis pattern is significantly attenuated in mitotic compared to interphase U266 cells as observed following: (A) microfluidic delivery of fl-tRNAs or (B) OPP tagging of nascent proteins in U266 with Click-iT AF488 protein synthesis kit. The clustering patterns of fl-tRNAs disappeared in mitotic cells (A, white arrows). Instead, the fl-tRNAs were scattered throughout the cytosol (A, lower panel). This observation aligns with a known fact that protein synthesis rate drops significantly in mitotic cells; Similarly, in non-mitotic cells, nascent proteins were mostly localized to form clustering patterns outside nucleus (B, upper panel), whereas for mitotic cells (B, white arrows, lower panel) the cluster disappeared, indicating a significantly decrease in protein synthesis in mitotic cells. The results from the two independent methods collectively confirmed a significant attenuation of protein synthesis activity in mitotic U266 cells. Scale bar: 5 µm.

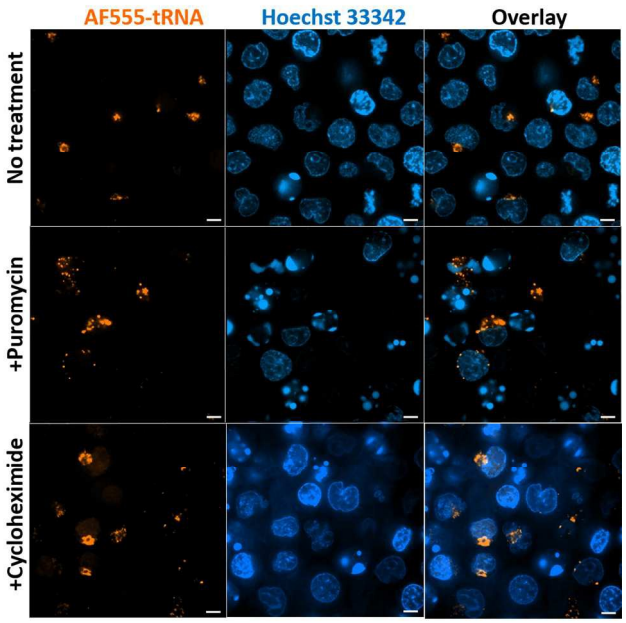

Figure 5 Effects of drug treatment on fl-tRNA localization. Puromycin treatment (2mM for 4 hours) altered the localization of AF555-tRNA, indicating that the delivered fl-tRNAs were functional and not randomly aggregating. Cycloheximide (0.1 mg/mL for 4 hours) did not have similar effects on changing fl-tRNA localization. Scale bar: 5 µm.

Integrative Biology Accepted Manuscript

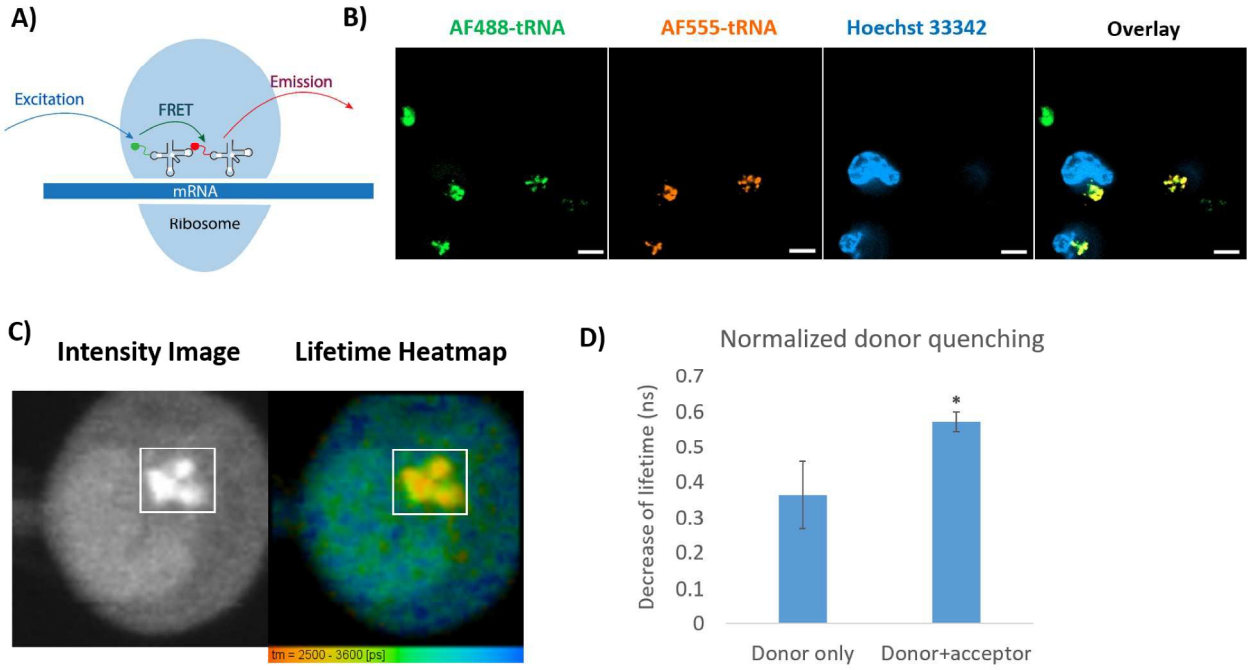

Figure 6 Protein synthesis activity mapped out in single live U266 cells by FLIM-FRET. AF488- and AF555-tRNAs or AF488-tRNAs alone were delivered into U266 cells and imaged 4 hours after transfection. (A) A schematic illustration of FRET generation by fl-tRNAs is shown; (B) co-delivered AF488- and AF555-tRNAs were highly colocalized and formed clustering pattern; (C) fluorescence lifetime scanning of a cell transfected with both fl-tRNAs showed a significantly decreased fluorescence lifetime of AF488 in the cluster pattern (white square) compared to that of cytosol fluorescence, suggesting that the AF488-tRNAs are quenched in the cluster; (D) quantification of the decrease of fluorescence lifetime inside the cluster pattern, normalized against cytosol fluorescence lifetime for cells transfected with both tRNAs or AF488-tRNAs alone; for each group, n=3; * $p<0.01$. Scale bar: 5 µm.

Integrative Biology Accepted Manuscript

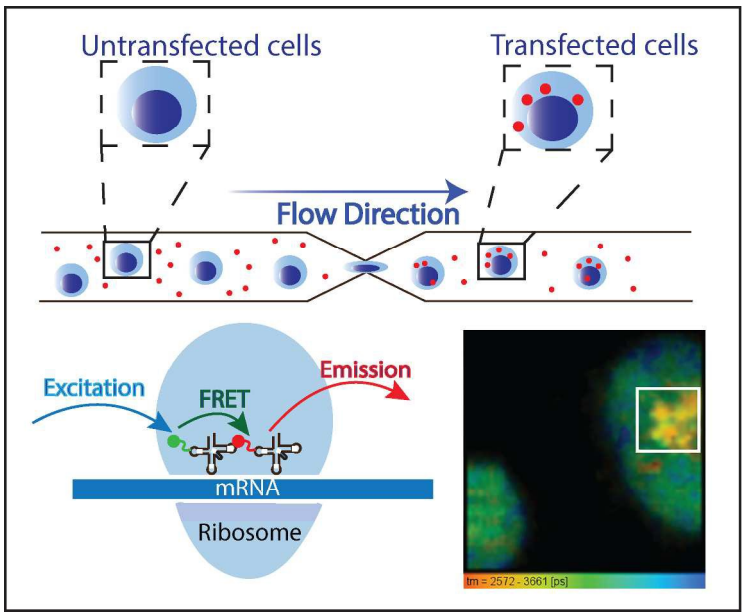

Microfluidic delivery of fluorescent tRNAs into hard-to-transfect cancer cells to map the protein synthesis activity in single live cells.

Integrative Biology Accepted Manuscript